Total energies and bonding for crystallographic structures in titanium-carbon and tungsten-carbon systems

David L. Price and Bernard R. Cooper
Department of Physics, West Virginia University, Morgantown, West Virginia 26506
(Received 7 July 1988)

A full-potential linearized muffin-tin orbital calculation is presented of titanium-carbon systems in a variety of crystallographic forms. The calculated electronic structure, total energies, and equilibrium lattice constants are determined for the ground-state NaCl structure of TiC and for prototype superlattice structures, and these results are discussed in terms of the nature of bonding found in TiC. Similar calculations are also given for WC in two of these crystalline forms, and the differing ground-state structure and equilibrium lattice constants in these two carbide materials are related to the behavior of those metallic *d* states which are occupied in WC and unoccupied in TiC. The behavior of these one-electron states, which stabilize WC in a simple hexagonal form, is similar to the calculated behavior of associated states in the prototype superlattice Ti-C structures, and these states are found to play a similar role in determining the structural characteristics in these systems. Some of the properties and probable stability of the various crystalline forms are also discussed in terms of our results.

I. INTRODUCTION

The transition-metal carbide compounds have long attracted interest both because of their striking mechanical properties and because of the somewhat unusual form of bonding observed in these materials. In general, the carbides exhibit extreme hardness and brittleness typical of materials which are covalently bonded, while still maintaining a degree of metallic electrical and thermal conductivity. Their melting temperatures are considerably higher than the metallic constituents alone and place them well among the refractory materials. This combination of properties has made the carbides important in a wide variety of technological applications, and the light weight of TiC has made it particularly attractive for aerospace applications. The rare combination of strong bonding and metallic conductivity has attracted theoretical attention to the electronic structure of these carbides, and calculations of both the pure crystals and the common substoichiometric forms have been extensive.[1–8] Recently, superlattices of metal carbides have been studied[9] with the aim of either developing improved properties, such as surface catalytic activity or resistance to corrosion, or finding new applications such as x-ray mirrors. The question then arises as to which other lattices of metal-carbon might be stable or metastable and what might their properties be.

The ground-state crystalline form of TiC, and other group-IV*B* metal carbides, is the rocksalt or NaCl structure. These carbides, in practice, are often not stoichiometric, but contain carbon vacancy defects, and the group-IV*B* carbides are stable in the NaCl form over a large range of fractional carbon content, titanium-carbon being stable[10] from TiC to $TiC_{0.5}$. The electronic structure and bonding in these cubic carbides have received much theoretical attention in both the stoichiometric[1–6] and nonstoichiometric[7,8] compositions, and, while there initially had been some debate about the form of bonding in these cubic carbides, it is now well established that the dominant contribution to cohesion comes from covalent bonds between carbon 2*p* states and the metal's *d* states, with secondary contributions from what is best described as metallic bonding and ionic bonding.

As one moves across the periodic table to the group-V*B* elements (V, Nb, and Ta), the cubic structure still exists over a large range of atomic fraction of carbon; however, the hexagonal form M_2C is found in a narrow range about its stoichiometric composition. Next, the group-VI*B* (Cr, Mo, and W) carbides are generally less stable, with simple carbides either being simply nonexistent, as in Cr, or showing a reduced range of nonstoichiometry in which the structures are stable. W_2C shows a relatively wide range of stoichiometry in which the hcp form is stable, while WC forms in a simple-hexagonal (D_{3h}) structure in a narrow range of carbon fraction near the stoichiometric ratio. The cubic, rocksalt form is not observed in the group-VI carbides at room temperature, although cubic WC has been observed at high temperatures (above 2500 °C).[11] Further along the transition-metal series, stable forms of simple-metal carbides are not observed.

The structural forms observed in the group-IV-VI transition-metal carbides suggest a natural progression from rocksalt TiC toward forming titanium-carbon superlattices, and we have performed self-consistent, full-potential linearized combination of muffin-tin orbitals (LMTO) calculations of the electronic structure and total energies of both TiC and WC in this series of crystallographic forms. It is of interest to compare TiC to WC in these calculations because WC is the one carbide observed to exist in the first three of the forms described above; and since the Ti-C superlattices naturally exhibit increased metallic bonding, the two extra valence elec-

trons of WC help illustrate the role of metallic bonding in stabilizing such atomic arrangements. The first structure which we shall examine here is the NaCl structure for both TiC and WC. The rocksalt form of TiC has been well studied[1-6] and our results for this are presented here largely to form a comparative basis for the other structures. The second structure examined (again for both TiC and WC) is the simple-hexagonal D_{3h} arrangement found in stoichiometric WC. This structure can be thought of as the simplest possible superlattice of TiC (i.e., a prototype for longer-period superlattices) with one layer of close-packed Ti stacked on one close-packed layer of C in an *AB* stacking. (Thus this structure would be simply hexagonal close packed if the two constituents were of the same type.) This structure can also be viewed as a deformed NaCl structure, in that it is possible to move from the NaCl structure to the hexagonal one by sliding the (111) planes of the rocksalt structure, containing either titanium or carbon, from an *ABC* stacking to an *AAA* stacking for one and to a *BBB* stacking for the other.

This rudimentary "1×1" superlattice shall form the basis for the construction of our two longer-period superlattices. Stacking *AB* layers of titanium on *C* layers of carbon gives a "2×1" superlattice and this is essentially the form of the M_2C carbides observed with group-V and -VI transition metals. Proceeding to *AB* layers of titanium on *AB* layers of carbon gives our final form, a "2×2" superlattice.

In Sec. II of this paper we briefly describe our full-potential LMTO calculational method, while in Sec. III we cover the calculated results for both TiC and WC in the rocksalt structure. In Sec. IV we deal with TiC and WC in the hexagonal D_{3h} structure, and in Sec. V we examine the multiple-layer superlattices. The final section contains a brief discussion and conclusions.

II. METHOD OF CALCULATION

Our method of solving the bulk density-functional problem is based on the LMTO formulation of Andersen,[12] where the program used here has a true interstitial region (not an atomic-sphere approximation) and incorporates a full-potential rather than a muffin-tin approximation. This section contains a brief description of the method.

The prescription for the complete potential is similar to that of other full-potential methods[13] that have been developed recently. Space is divided into touching spheres, centered on the sites of nuclei, and the remaining interstitial region. Inside the spheres the potential is expressed as a sum of lattice harmonics,

$$V_\alpha(\mathbf{r})=\sum_h V_{\alpha,h}(r)D_{\alpha,h}(\hat{\mathbf{r}}) , \tag{1}$$

where the functions $D_{\alpha,h}(\hat{\mathbf{r}})$ are the lattice harmonics invariant under point-group operations and α runs over inequivalent spheres in the unit cell. In the interstitial region the potential is expressed as a Fourier series,

$$V_i(\mathbf{r})=\sum_{\mathbf{G}} e^{i\mathbf{G}\cdot\mathbf{r}}V(\mathbf{G}) . \tag{2}$$

The zero of potential is set so that the average potential in the interstitial region is zero. The ratio of the radius of the carbon spheres to those of the titanium or tungsten spheres is chosen so that, in the NaCl structure near the equilibrium lattice constant, the spherical averages of the self-consistent potential are equal on the surface of the muffin-tin spheres for the two constituent species. These ratios are then kept constant as the lattice parameters and crystal structure are varied.

Given an input potential expressed as above, the LMTO calculation proceeds by first forming a muffin-tin potential from the true potential (spherically averaged in the spheres and zero in the interstitial region), and then using this muffin-tin potential to construct basis states. These states are defined as the Bloch sum,

$$\Psi^{\mathbf{k}}_{\kappa,\alpha,L}(\mathbf{r})=\sum_{\mathbf{R}} e^{i\mathbf{k}\cdot\mathbf{R}}\Phi_{\kappa,\alpha,L}(\mathbf{r}-\rho_\alpha-\mathbf{R}) , \tag{3}$$

where L represents both l and m quantum numbers and ρ_α is the position of the αth sphere in the unit cell. The "muffin-tin orbitals" Φ are (with some subscripts suppressed)

$$\Phi_{\kappa,\alpha,L}(\mathbf{r})=\begin{cases}[A\phi_{\kappa,\alpha,l}(r_\alpha)+B\dot{\phi}_{\kappa,\alpha,l}(r_\alpha)]Y_L(\hat{\mathbf{r}}) & \text{in the } \alpha\text{th muffin tin at } \mathbf{R}=\mathbf{0} ,\\ [-\kappa^{l+1}n_l(\kappa r)]Y_L(\hat{\mathbf{r}}) & \text{in the interstitial} ,\\ \sum_{l'}^{l_{\max}}\sum_{m'}[C\phi_{\kappa,\beta,l'}(r_\beta)+D\dot{\phi}_{\kappa,\beta,l'}(r_\beta)]Y_{L'} & \text{in all other spheres} .\end{cases} \tag{4}$$

The functions $\phi(r)$ are solutions of the semirelativistic Dirac equation[14] and the $\dot{\phi}(r)$'s are the energy derivatives of these, all evaluated at chosen energy parameters $E_{\kappa,\alpha,l}$. The coefficients $A-D$ are chosen to make the basis states continuous and to have continuous first derivatives. The Y_L are spherical harmonics, and $n_l(\kappa r)$ is a Neumann function of kinetic energy κ^2 (or a Hankel function if κ^2 is less than zero). While the computer program is capable of including spin-orbit matrix elements in the Hamiltonian, we have omitted them here. Each value of the parameter κ is associated with a separate "energy window," allowing coverage of the various subbands. The energy parameters $E_{\kappa,\alpha,l}$ are either set at the center of mass of the occupied band (for narrow bands) or at the center of mass of the muffin-tin-sphere-energy-window l-projected energies (except where orthogonality to core states had to be

maintained). The values of κ^2 were, as a rule, set to the interstitial, window-projected energies. These parameters are reset at each iteration as are the basis functions. This method of choosing the various parameters has been found in a number of tests to reliably give those values which minimize the total energy. The core states, not included in the valence set, are solutions of the full Dirac equation in the spherically averaged potential in each sphere. The value of $l_{\max}$ in Eq. (4) was kept at 3.

The basis states used were $2s$, $2p$, and $3d$ on the carbon sites and $3p$, $4s$, $4p$, $3d$, and $4f$ on the titanium sites, with separate energy windows for the C $2s$ band and the Ti $3p$ band, and Ti $4s$, $4p$, $4p$, $4d$, and $4f$ states in the same window as the C $2p$ and $3d$ states. For W, the corelike $5p$ states, corresponding to the Ti $3p$ states, were not included in the valence basis set, thus giving two energy windows for the tungsten carbides rather than three windows as in the titanium carbides.

The Bloch sum [Eq. (3)] is evaluated in the spheres using calculated structure functions[15] (recalculated at each iteration as the energy parameters are reset) and in the interstitial region by expanding the sum of Neumann functions, each with an arbitrary, smooth extension into the muffin-tin spheres in a Fourier series. The construction of the Hamiltonian matrix elements is then performed either by analytic expressions or simple radial integrals in the spheres and by convolution with a step function in the interstitial region, with care taken to include the necessary number of Fourier components in the step function. The overlap matrix is constructed in a similar manner and the diagonalization of the Hamiltonian follows standard techniques. It should be pointed out that our energy windows are allowed to hybridize; that is, matrix elements connecting basis functions associated with different sets of energy parameters are included in the construction of the Hamiltonian and overlap matrix elements. The representative points in the Brillouin zone are chosen according to the special-points scheme.[16] Ten special points were used in the irreducible $\frac{1}{48}$ portion of the Brillouin zone for the NaCl structure and 12 points in the irreducible $\frac{1}{24}$ part of the Brillouin zone for the simple-hexagonal structure. For hexagonal structures of lower symmetry, 12 points in the irreducible zones were also used. The determination of the Fermi level is straightforward, and the electron density is constructed into a form analogous to the expression for the potential. Core charge which leaks from the muffin-tin spheres is added to the charge density in the interstitial and other muffin-tin spheres by Fourier synthesis of the tails which extend beyond the sphere edge.

The computation of the potential, given the density, consists of finding the electrostatic potential and the exchange and correlation potential (we use the exchange and correlation potential of Ceperly and Alder[17] as parametrized by Perdew and Zunger[18]). The electrostatic potential is found using the method of Weinert.[19] The exchange and correlation potential is found in the interstitial region by Fourier transforming the charge density from reciprocal to real space and then backtransforming the potential. The exchange and correlation potential is found in the muffin-tin spheres using a simple numerical angular integration scheme. The input and output potentials are then mixed using Broyden's mixing scheme,[20] which we found to give quick convergence to self-consistency

The total energy,

$$E = T + E_H + E_{\rm xc} = \sum_i \varepsilon_i - \int \rho(\mathbf{r}) V_{\rm eff}(\mathbf{r}) + E_H + E_{\rm xc} \ , \tag{5}$$

is calculated using the cancellation of the Z/r terms[21] between the kinetic energy T and the electrostatic (Hartree) energy E_H, and the input value for the one-electron potential, $V_{\rm eff}(\mathbf{r})$, is used in Eq. (5) so as to obtain quick convergence of the total energy. $E_{\rm xc}$ is the net exchange and correlation energy and is calculated in a manner similar to the construction of the exchange and correlation potential. Cohesive energies are obtained using a fully relativistic calculation of the associated atomic energies, using numerical procedures which are as similar to those of the LMTO calculation as possible.

The total and muffin-tin-sphere l-projected densities of states were calculated on a tetragonal mesh,[22] using 89 points in the irreducible potion of the Brillouin zone for the cubic systems and 64 in the irreducible $\frac{1}{24}$ of the Brillouin zone in the simple-hexagonal structure. For hexagonal lattices of lower symmetry, this set of 64 points was expanded by the appropriate symmetry operations to the remaining portions of the irreducible zone.

III. NaCl STRUCTURE: TiC AND WC

The NaCl structure is observed to be the ground-state form of TiC, and a number of band calculations of its electronic structure have been presented previously. The conclusion of this series of work is that bonding in cubic TiC is dominated by covalent bonds between C $2p$ and Ti $3d$ states of the type shown schematically in Fig. 1. The p—d σ bonds with e_g-symmetry d states form the strongest bonds, while the p—d π bonds, and to some extent metallic d—d bonds as well, also play a role in the electronic bonding. While a limited amount of metallic d—d bonding and ionic bonding (due to charge transfer from titanium to carbon) have been identified in TiC, it is clear that it is the octahedral form of the covalent-bonding arrangement which determines the NaCl structure as the ground state. A good demonstration of this bonding is given by the muffin-tin l-projected density of states (DOS). Our calculated results for the major components of the projected density of states are given in Fig. 2 and are in agreement with published results. The total density of states is given in Fig. 3.

As seen in Fig. 2, the C $2s$ states form a narrow, isolated band about 0.3 Ry below the C $2p$–Ti $3d$ valence band, with a small admixture of Ti d character. C s-p hybridization plays no role in the bonding here. The C $2p$ and Ti $3d$ states form a wide band centered about the Fermi energy and the C $2p$ and Ti $3d$ characters of the states below the Fermi energy are both large and show a strong correlation, indicating substantial bonding between these orbitals. The remainder of the valence states

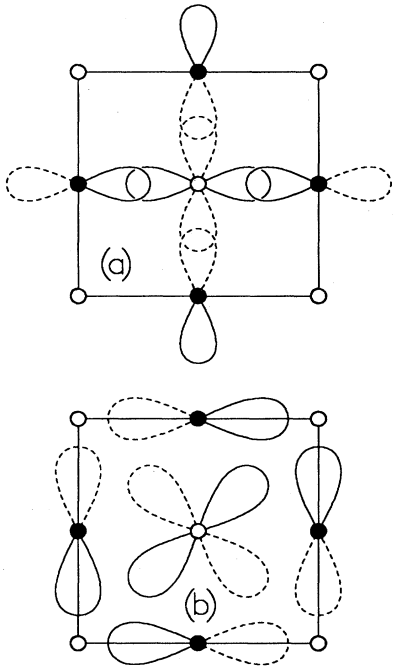

FIG. 1. Schematic diagram of the form of metal $d-Cp$ covalent bonds in (100) plane of the rocksalt structure (after Ref. 4). Diagram (a) shows σ bonds when the metal's d states have e_g symmetry, and (b) the π bonds with metallic states of t_{2g} symmetry. The solid and dashed lines indicated regions of opposite sign.

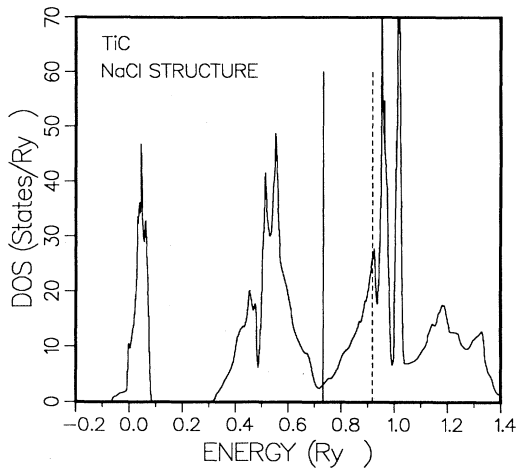

FIG. 3. Total density of states for TiC in the NaCl structure. The vertical solid line indicates the Fermi energy, while the dashed line gives the Fermi energy that would accommodate two more electrons per unit cell.

are separated by a wide gap from the occupied states, again indicating strong covalent behavior. These unoccupied states are largely of Ti d character and have been identified[4] as either C $2p$ – Ti $3d$ antibonding states or metallic Ti d states of, in general, either nonbonding or antibonding character. The Fermi energy itself falls at the bottom of a wide minimum in the DOS with a density of states at E_F of 3.16 states/Ry. Thus, rocksalt TiC, with six valence electrons (excluding the C $2s$ band), succeeds in filling all of the available bonding states while leaving the remaining states unfilled, resulting in a strong and stable structure. Moving to the group-V and -VI transition metals, a simple rigid-band model would predict that the additional electrons must fill more of the high-energy "antibonding" orbitals and, as a consequence, these compounds are increasingly unstable in the NaCl form. WC has two more electrons per unit cell than TiC, and Fig. 3 shows that the Fermi level that would accommodate these two extra electrons lies near a large peak in the Ti $3d$–projected density of states, and so WC falls at a point where the destabilizing effects of these states becomes critical. These predictions regarding the electronic structure of WC are to be compared to the calculated density of states of cubic WC given below.

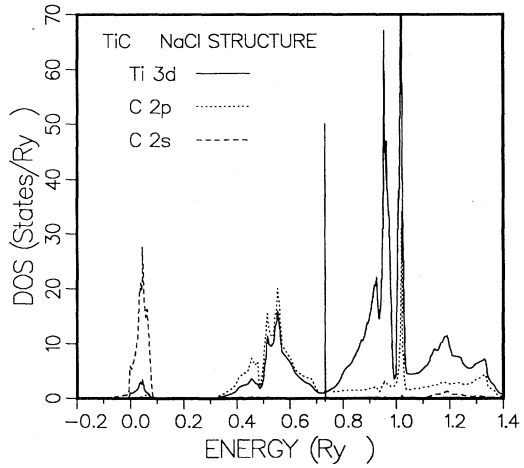

FIG. 2. Muffin-tin-sphere l-projected density of states in TiC in the NaCl structure. Only the T d-, C p-, and C s–derived densities are shown. The vertical solid line shows the Fermi energy.

The calculated total energy of rocksalt TiC serves as a basis for comparison to the other structures, and the calculated total energy versus lattice constant is given in Fig. 4. The calculated points were fitted by least squares to a cubic polynomial (the maximum deviation from the fitted curve was 8.6×10^{-5} Ry; a quartic fit gave essentially the same results) and the predicted lattice constant, given in Table I, is in good agreement with experiment. The cohesive energy, 8.89 eV per atom, as is typical of local-density-functional calculations, is about 26% too large. The relatively large bulk modulus of 2.14 Mbar, more that twice that of bulk Ti, 1.05 Mbar, and the large cohesive energy are again consistent with the strong bonding revealed in the electronic density of states.

The NaCl structure is not observed in the group-VI transition-metal carbides at room temperature, although it has been observed in WC above temperatures above 2500 °C. Figure 5 shows the l-projected and total density of states for WC in the NaCl structure (with a lattice con-

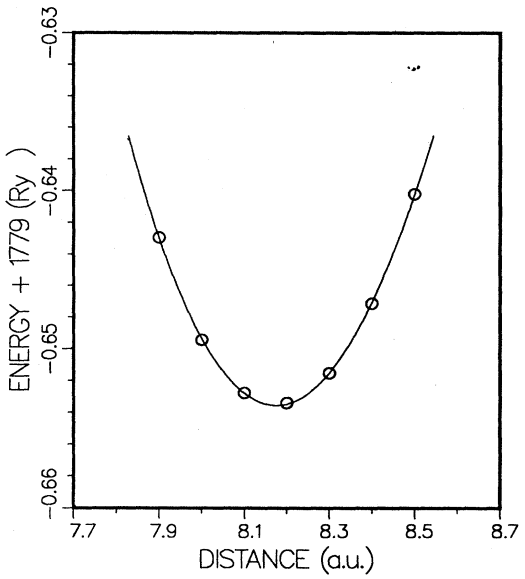

FIG. 4. Total energy per unit cell of TiC in the rocksalt structure as a function of the lattice constant a, the length of the conventional cube edge. The solid curve is a cubic fit to the calculated energies.

stant of 8.1 a.u.), and the rigid-band prediction based on Fig. 3 appears to be quite accurate. The Fermi level has indeed moved up to a point where the W $5d$-projected density of states is large, implying that a rearrangement of the lattice might well lower the total energy. The C $2s$ band has widened compared to that of TiC (to approximately 0.2 Ry from 01 Ry), but remains isolated from the higher C $2p$–W $5d$ band. This higher band still exhibits the same tight p-d correspondence as between the C $2p$ and Ti $3d$ states, so a large degree of p—d bonding remains.

Figure 6 shows the calculated total energy of rocksalt WC versus lattice constant. The calculated minimum in Fig. 6 is is at $a=8.10$ a.u. The calculated cohesive energy and bulk modulus are given in Table I and are discussed further in the next section. (We tested here the sensitivity of both the calculated equilibrium position and the bulk modulus to the number of data points used in the fit, by fitting to both five points and nine points—the change in both quantities was less than 1%.) Experimental data for WC in this high-temperature form is sparse. The equilibrium lattice constant has been measured[24] at 7.86 a.u. for $WC_{0.5}$ and at 7.97 a.u. for $WC_{0.82}$, and a linear extrapolation of these results to WC gives a value of 8.02 a.u. It should be noted that the calculated equilibrium lattice constant is quite close to that of TiC and in reasonably good agreement with the experimental value.

IV. SIMPLE-HEXAGONAL STRUCTURE: TiC AND WC

The simple-hexagonal structure depicted in Fig. 7 is the observed crystalline form of stoichiometric WC up to very high temperatures and is unobserved in TiC. As mentioned in the Introduction, this structure is a stacking of A layers of titanium on B layers of carbon and can be thought of as a one by one superlattice of close-packed layers of metal atoms on layers of carbon atoms. Both

TABLE I. Summary of calculated parameters of each system, with comparisons to experiment where available.

System	Lattice constants (a.u.)	Cohesive energy (eV/atom)	Elastic constants[a]	DOS at E_F (states/Ry)
TiC (NaCl)	8.18	8.89	$B=2.14$	3.16
Expt:	8.182[b]	7.04[c]	$B=2.42$[c]	
WC (NaCl)	8.10	9.46	$B=3.19$	14.53
Expt:	8.02[d]			
TiC (hex.)	$a=5.84$	8.11	$B=2.31$	2.17
	$c=5.02$		$Y_z=3.18$	
			$\sigma_{xz}=0.387$	
WC (hex.)	$a=5.44$	9.72	$B=3.29$	3.23
	$c=5.33$		$Y_z=8.48$	
			$\sigma_{xz}=0.121$	
Expt:	$a=5.492$[c]	8.34	$B=3.31$[c]	
	$c=5.361$			
Ti_2C	$c=9.17$	8.03	$\partial^2E/\partial^2c=0.76$ (Ry)/a.u.^{2}	25.99
Ti_2C_2				
$d_3=4.50$		4.80		37.33
$d_3=1.83$		6.92		68.65

[a] B, bulk modulus (Mbar); Y_z, Young's modulus (Mbar); σ_{xz}, Poisson's ratio.
[b] Reference 23.
[c] Reference 10.
[d] Reference 24.

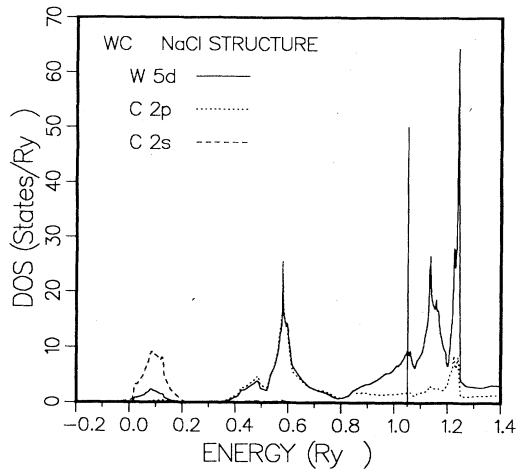

FIG. 5. Muffin-tin-sphere l-projected density of states calculated for WC in the NaCl structure.

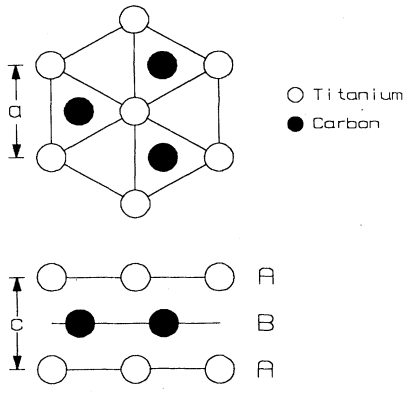

FIG. 7. Hexagonal (D_{3h}) structure, drawn with $c/a=1$.

types of atom in this lattice have D_{3h} point symmetry and the irreducible portion of the Brillouin zone is then $\frac{1}{12}$ of the full zone. Using time-reversal symmetry, the special **k** points can be confined to $\frac{1}{24}$ of the Brillouin zone and 12 such points were used.

Converged results for TiC in this structure were obtained over a range of values of the c and a lattice constants (at 24 pairs of values from $c=4.7-5.7$ a.u. and $a=5.3-6.1$ a.u.), and the projected density of states with the lattice constants near their minimum-energy values is shown in Fig. 8. Figure 9 gives the calculated total density of states. The states below the Fermi energy are qualitatively similar to those of cubic TiC. In particular, the C 2s band remains narrow and isolated and the C 2p and Ti 3d densities remain closely correlated, indicating that the covalent bonds between these states remain intact. It should be noted that this remains so in spite of the fact that the octahedral environment of the carbon atoms in the NaCl structure is broken in this hexagonal structure. In the NaCl form the six titanium nearest-neighbor atoms of a given carbon atom, when viewed along the perpendicular to the (111) planes, form two equilateral triangles (Fig. 10) inverted with respect to each other. Given the c/a ratio of the NaCl form, the carbon atoms then sit at octahedral sites, with the carbon atoms directly in line with pairs of titanium atoms and all of the acute Ti—C—Ti bond angles being 90°. This allows formation of the type of covalent bonds depicted in Fig. 1. In the simple-hexagonal structure, the six titanium nearest neighbors of the carbon atoms, viewed along the c axis, are arranged in pairs of aligned triangles, and thus the carbon atoms do not sit along lines joining titanium atoms and all of the acute Ti—C—Ti bond angles cannot be simultaneously brought to 90°.

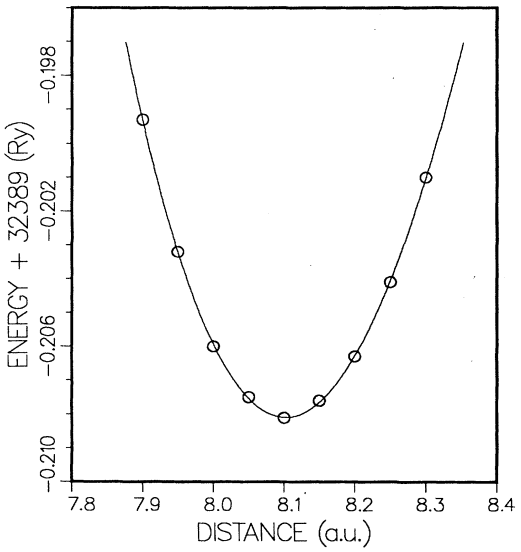

FIG. 6. Calculated total energy of WC in the NaCl structure as a function of a, the length of the conventional cube edge. The solid curve is a cubic fit to the calculated energies.

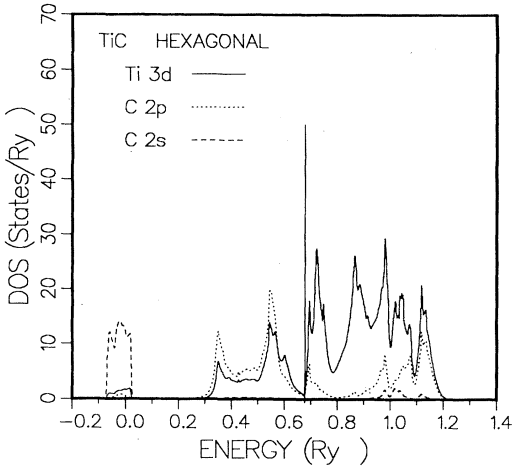

FIG. 8. Muffin-tin-sphere l-projected density of states for TiC in the hexagonal structure with lattice constants $a=5.9$ a.u. and $c=4.9$ a.u.

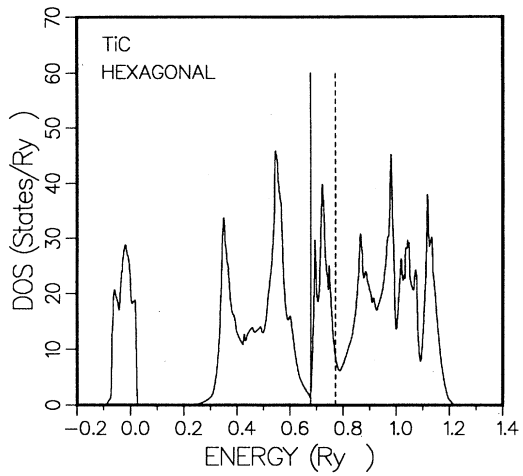

FIG. 9. Calculated total density of states for TiC in the hexagonal structure. The solid vertical line shows the Fermi energy, and the dashed vertical line shows the Fermi energy that would contain two more electrons per unit cell.

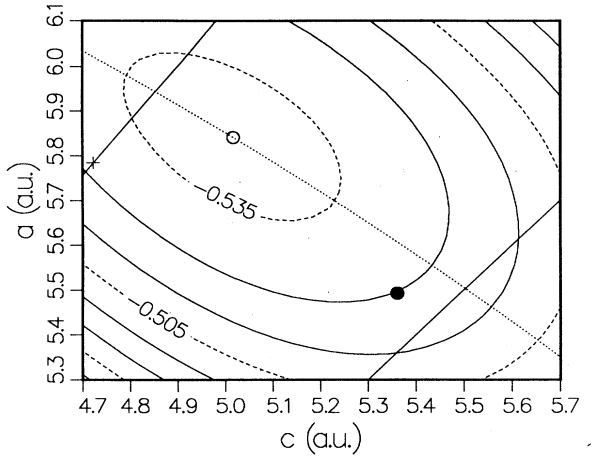

FIG. 11. Contour plot of a two-dimensional polynomial fitted to the calculated total energies in the *c-a* plane for TiC in the hexagonal structure. The open circle indicates the minimum in the fitted surface and the dotted line shows those points which have the same Ti-C distance as at this minimum. The solid circle lies at the experimental lattice constants of hexagonal WC. The points on the upper solid line all have the c/a ratio of the NaCl structure and the + symbol on this line is the point which corresponds to the calculated lattice constant of TiC in the NaCl structure. The lower solid line is that of $c=a$.

The Fermi energy now falls into a narrow minimum in the density of states, with the density of states at the Fermi level having a value of 2.18 states/Ry. The states above the Fermi level, particularly the metallic 3*d* states, have changed markedly from their distribution in the NaCl structure, with a number of additional peaks in the density of states having been created. The density of states rises rapidly above the Fermi level and a pronounced minimum has formed only about 0.12 Ry above the Fermi energy. Again, if the Fermi energy were moved up enough to accommodate tungsten's two additional electrons, it would fall within this sharp minimum in the density of states and thus single-particle states of lower energy could be occupied in this form for WC than in the NaCl form. A group-V transition metal, also never observed in this form, would have its Fermi energy nearly on the peak which separates these two minima.

A two-dimensional polynomial including terms up to third order in *c* and *a* was fitted to the calculated total energies with a maximum deviation of 2.8×10^{-3} Ry. In Fig. 11 this fitted polynomial for the total energy of hexagonal TiC is given as a contour plot in the *c-a* plane, and a number of features are of interest. The minimum is found at the point $c=5.02$ a.u. and $a=5.85$ a.u., in this case differing substantially from the experimentally obtained values for WC (also shown in Fig. 11). The energy at this minimum is -1779.5383 Ry per cell, which is 0.78 eV per atom above the minimum energy calculated for the rocksalt structure. This, of course, is in agreement with the observation that TiC forms in the NaCl structure. Evaluating the second derivatives of the fitted polynomial at the minimum gives values for the bulk modulus, Young's modulus, and Poisson's ratio which are listed in Table I.

Also indicated in Fig. 11 is the (dotted) line passing through the minimum which has a constant value of the Ti-C nearest-neighbor distance (which is also close to a line of constant volume). It can be seen that the total energy increases steeply away from this line and is relatively shallow along it, indicating that compression or extension of the covalent bonds is resisted. The upper solid line in Fig. 11 (toward the upper left-hand corner) indicates those points which have the same c/a ratio as a rocksalt lattice and so can be obtained from a rocksalt lattice by sliding the (111) planes as discussed in the Introduction. The + symbol on this line shows the lattice constants obtained if the hexagonal structure were created by simply sliding rocksalt TiC from its calculated equilibrium lattice constant. At this point the Ti-C distance is the same as in the NaCl form, 4.09 a.u., and by moving from there to the equilibrium values of *c* and *a*, at which the Ti-C distance is slightly larger at 4.19 a.u., the system lowers its energy by about 0.011 Ry. The small increase in the Ti-C distance is indicative of a weakening of the metal–carbon bonds in this structure.

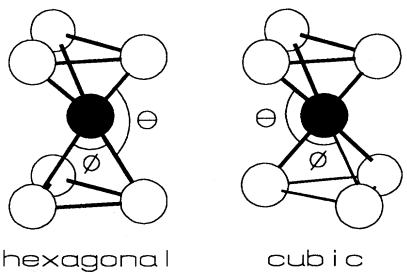

FIG. 10. Arrangement of a carbon atom's six nearest titanium atoms in the hexagonal and rocksalt structures. In the rocksalt structure both angles ϕ and θ are 90°.

In the NaCl form the Ti-Ti distance is 5.78 a.u., expanded by about 6% from the bulk titanium (hcp) nearest-neighbor distance 5.47 a.u. In the hexagonal structure, however, the (111) planes of titanium lie on top of each other and, at the "slid" position, the Ti-Ti separation is reduced to 4.723 a.u., the value of the c lattice parameter. The a lattice parameter in this position is 5.784 a.u. At the equilibrium position the c lattice parameter has expanded to 5.02 a.u. and so the Ti-Ti distance remains 8% smaller than the bulk value and 13% smaller than in NaCl-form TiC.

One last point to be made about the equilibrium c and a lattice constants concerns the bond angles as functions of c and a. Along the upper solid line in Fig. 11, the three Ti—C—Ti bond angles from the carbon sites to the three titanium sites in either (111) plane are all still 90°, although the acute bond angles joining titanium sites in adjacent (111) planes are reduced to 70.5°. The lower solid line in the c-a plane indicated in Fig. 11 (toward the lower right-hand corner) shows the points where the c/a ratio is equal to 1. When $c/a=1$, all of the acute Ti—C—Ti bond angles are equal at 81.8° and, in this respect, the hexagonal structure has recovered the octahedral environment of the carbon atoms as closely as possible. As this line is close to the experimental lattice constants of hexagonal WC, it might have been assumed that this configuration optimizes the covalent interaction in this structure. However, it can be seen that for hexagonal TiC the calculated equilibrium position lies somewhat closer to the upper solid line, where the pair of acute angles θ and ϕ, shown in Fig. 10, are $\theta=73.3°$ and $\phi=88.0°$. Thus the calculated values of the lattice constants c and a roughly maintain the Ti—C bond length while giving a Ti-Ti distance about 0.8 a.u. smaller than that in bulk Ti.

The corresponding calculation for WC in this form was performed and the projected density of states at the lattice constants $c=5.4$ a.u. and $a=5.5$ a.u., near the experimental values ($c=5.36$ a.u., $a=5.49$ a.u.), is presented in Fig. 12, and compares reasonably well with published results.[25] The C 2s band has recovered its narrow width compared to the results for rocksalt WC and, again, the covalent bonds between the C 2p and W 5d states appear to persist. However, as suggested above in the discussion of hexagonal TiC, some states of the "d band" have moved lower in energy and the Fermi energy now falls near a minimum in the density of states. Apparently then, the hexagonal structure splits the metallic d levels into bonding and antibonding states (with a strong C p admixture) and the Fermi energy falls at a point where the eight valence electrons fill bonding states, leaving the corresponding high-energy antibonding states unfilled.

A third-order polynomial was again fitted to the calculated total energies and a contour plot of the fitted energy surface is given in Fig. 13 for the range of c and a covered. The maximum deviation from the fitted curve is 2.9×10^{-4} Ry. The minimum-energy lattice constants, $c=5.33$ a.u. and $a=5.44$ a.u., are within 1% of the experimental values and, unlike those of hexagonal TiC, fall near the line of $c/a=1$. The W-W distance, along the c axis, is 5.33 a.u., which is now slightly larger than the bulk, bcc tungsten nearest-neighbor distance of 5.172 a.u., while the W—C bond length is 4.11, again nearly equal to that calculated for NaCl-structure WC (4.05 a.u.). As can be seen in Fig. 13, the long axis of the constant-energy ellipses is visibly shifted away from the line of constant W—C bond length and is shifted so that it is more closely parallel to the c axis in the c-a plane. This can also be seen in the much smaller value for Poisson's ratio (Table I) than in hexagonal TiC. All of these observations point to the conclusion that tungsten's two additional d electrons (compared to titanium), engaging in W—W metallic bonding rather than in W—C covalent bonds, tend to force the nearest-neighbor W—W separations to values similar to those found in bulk W (thus largely pulling in the six W nearest neighbors in the a layers), while simultaneous maintenance of the W—C

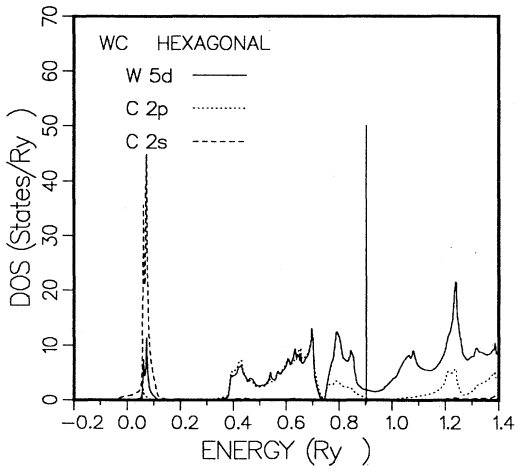

FIG. 12. Muffin-tin-sphere l-projected density of states for WC in the hexagonal structure.

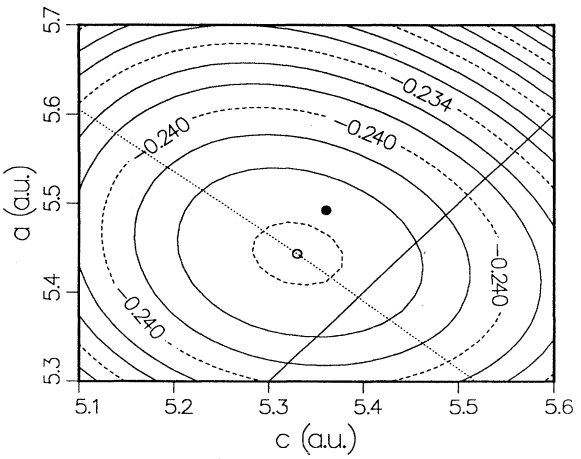

FIG. 13. Contour plot of a two-dimensional polynomial fitted to the calculated total energies in the c-a plane for WC in the hexagonal structure. The open circle indicates the minimum in the fitted surface and the dotted line shows those points which have the same W-C distance as at this minimum. The solid circle lies at the experimental lattice constants of hexagonal WC and the solid line is that of $c=a$.

bond length requires that the system move away from the c/a ratio of the rocksalt structure.

The total energy at the minimum is $-32\,389.2463$ Ry per unit cell, 0.26 eV (or 3018 K) per atom below the minimum energy in the NaCl structure. This agrees with the observation of the hexagonal form as the ground state of WC and is at least consistent with the observation[11] of the simple-hexagonal to NaCl transition temperature in stoichiometric WC at 3028 K.

V. TiC SUPERLATTICES

In this section we describe the titanium-carbon system in the two other forms investigated, one with two layers of titanium stacked on single layers of carbon and one with two layers of titanium on two layers of carbon, the second being our most advanced step in the progression toward Ti-C superlattices. In the "2×1" structure, sketched in Fig. 14, we take the titanium to be in *AB*-stacked close-packed layers followed by a carbon layer placed in the *C* sites. This arrangement, essentially the same as that found in the M_2C carbides (e.g., Ta_2C and W_2C) and not observed in Ti-C, again places the carbon atoms in the center of pairs of inverted triangles of titanium atoms and so, given appropriate choices for the a lattice parameter and the distance between carbon and titanium layers, gives the carbon atoms an octahedral environment. We have not, for the two structures described in this section, varied all of the available lattice parameters, but have followed a reasonable procedure in choosing them. Thus for the Ti_2C, 2×1 arrangement, we first require that the titanium-carbon nearest-neighbor distance is the same as in equilibrium NaCl titanium carbide (4.09 a.u.). Given this, the requirement that the carbon sites have octahedral coordination determines the a and d_1 distances shown in Fig. 14. The remaining parameter is the distance d_2 (since $c=2d_1+d_2$) separating adjoining layers of titanium. While we have calculated and shall discuss the variation of the total energy with respect to this distance, *a priori* it is reasonable to assume that the equilibrium value of this parameter will be such that the bulk titanium nearest-neighbor distance is recovered between the adjacent titanium layers. Following the same assumptions for W_2C would give the lattice parameters $a=5.671$ a.u., $d_1=2.315$ a.u., and $d_2=4.004$ a.u., and these compare well with the experimental values[24] of 5.654, 2.419, and 4.085 a.u., respectively, suggesting that this choice of parameters in Ti_2C is close to optimum. The titanium sites in this lattice have C_{3v} point symmetry, having lost the reflection symmetry along the c axis present in the simple-hexagonal structure of the preceding section. The carbon sites are centers of inversion symmetry giving them D_{3d} symmetry, and the two titanium atoms in each unit cell, by this inversion operation, are equivalent.

From this "2×1" lattice follows the "2×2" lattice in which the stacking is *AB* for two layers of titanium with two layers of carbon also in an *AB* arrangement as shown in Fig. 15. The carbon atoms now have only three titanium nearest neighbors as opposed to six in all of the other structures. Here we have fixed all of the lattice parameters and not optimized them by minimizing the calculated total energy. First, the titanium-carbon distance is again set to that of cubic TiC and the distances from the titanium to carbon layers and the a lattice parameter are then determined by requiring that the carbon sites be at the octahedral location with respect to the three nearest titanium atoms. The distance between the titanium layers, d_2 of Fig. 15, is kept at the value which minimized the energy of the Ti_2C lattice. This leaves only the distance between adjoining carbon layers undetermined and the calculated results for two choices of this distance are discussed below. Each of the atoms in this lattice have C_{3v} point symmetry, and the two titanium and two carbon atoms in the unit cell are equivalent by an inversion operation through the (unoccupied) *C*-layer stacking sites between either the carbon or titanium layers. (These points have D_{3d} point symmetry, and one served as the origin in the calculation.)

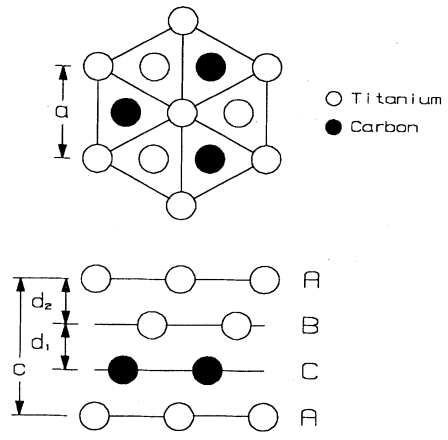

FIG. 14. This figure shows the structure chosen for the Ti_2C lattice. The distance a and d_1 are fixed as discussed in the text and the distance d_2 was varied.

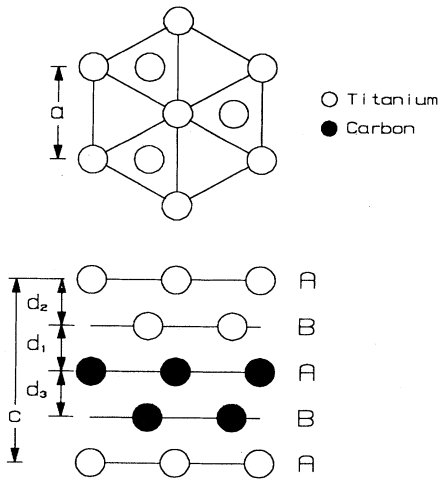

FIG. 15. The lattice used in the calculation for Ti_2C_2. The distance a, d_1, and d_2 were fixed and two values for d_3 were investigated.

Figure 16 contains the calculated total energy of the 2×1 Ti_2C structure as a function of the unit cell length c, and thus also as a function of the distance d_2 of Fig. 14. The minimum is found at a c lattice constant of 9.17 a.u., or $d_2=4.43$ a.u., which gives a Ti-Ti separation distance of 5.56 a.u. compared to the bulk Ti nearest-neighbor distance of 5.47 a.u. The second derivative $\partial E^2/\partial d_2^2$ is less than half that of $\partial E^2/\partial c^2$ for TiC in the hexagonal lattice and so is more of the magnitude to be associated with bulk Ti. The total energy at the minimum is not directly comparable to that of the previous two structures since here the number of titanium and carbon atoms in the unit cell are not equal; however, this lattice can be obtained from the simple-hexagonal lattice by removing every other close-packed layer of carbon atoms and rearranging the stacking sequence. The required energy per removed carbon atom in such a transformation is then 2 times the energy per unit cell of the simple-hexagonal lattice minus the energy of one unit cell of Ti_2C and a carbon atom at infinity. This calculated difference is 0.613 Ry. Since removing each carbon is analogous to breaking three chemical bonds with neighboring titanium atoms, this gives a rough estimate of the energy per covalent bond of 0.204 Ry (2.8 eV), which is consistent with the typical energy of a covalent bond. This estimate is on the low side, however, since the removed carbon atom takes with it only two valence (p) electrons and thus one remaining electron is free to form metallic d—d bonds.

The l-projected density of states is shown in Fig. 17. This figure shows that the occupied states in this arrangement have some similarity to the occupied states in simple-hexagonal WC. There is again the correlation between C p and Ti d densities in the states below about 0.55 Ry (containing six electrons per unit cell) associated with covalent bonds between these orbitals. The magnitude of the Ti d-projected density of states in this region,

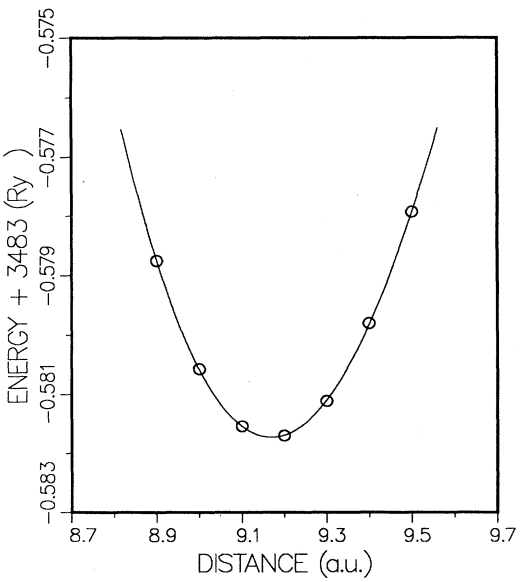

FIG. 16. The calculated total energy of Ti_2C as a function of the c lattice parameter of Fig. 14. The solid curve is a cubic fit to the calculated energies.

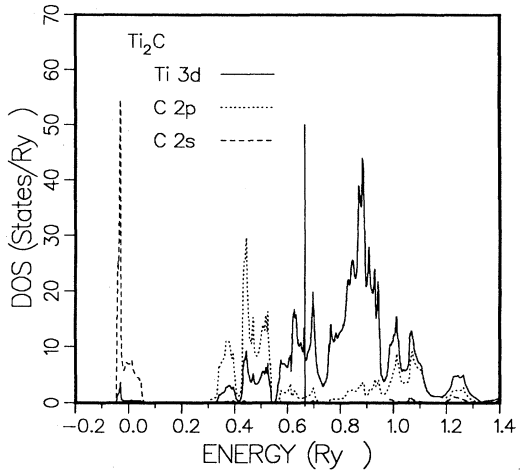

FIG. 17. Muffin-tin-sphere l-projected density of states for Ti_2C with a c lattice constant of 9.2 a.u.

relative to the C p-projected density, is here much smaller than in the hexagonal structure only because each Ti atom now has only three carbon neighbors, while each carbon atom still has six titanium nearest neighbors. (The Ti d-projected density of states shown is that projected onto the muffin-tin sphere of only one of the two equivalent titanium atoms.) Again, states of largely Ti d character have formed just above this covalent band and here are separated form the covalent states by a small gap. The total p-d valence band, with one more titanium atom than TiC, contains 10 electrons, and the largely metallic d states contain four electrons, just those which are not engaged in the covalent bonding. The Fermi level falls at a higher density of states, 25.99 states/Ry, than any of the previous forms of TiC (even given the simple fact that there are more atoms per unit cell), a value that begins to be comparable to the density of states at the Fermi level in bulk titanium. The unsurprising conclusion, from both the total energy and the density of states, is that the interaction between adjoining titanium layers is already quite similar to the metallic bonding of pure titanium. An interesting comparison can also be made between the calculated density of states of substoichiometric TiC of Ref. 8 and these results for Ti_2C. In Ref. 8, a supercell calculation of $TiC_{0.75}$ was described in which one of every four carbon atoms was removed from a rocksalt TiC lattice. The excess Ti d electrons, unable to form C—Ti covalent bonds, were found to form strong overlaps in the vacancy regions, again resulting in the formation of d-like states centered at the minimum in the DOS, just above the band of covalent p-d states. These "vacancy" states then provide states to fill that are lower in energy than those suggested by a rigid-band model, and this would seem to be closely related to the observation[10] that titanium-carbon with the chemical formula $TiC_{0.5}$ is stable, but in the NaCl form with carbon vacancies, rather that in the structure of our Ti_2C superlattice.

Next, we discuss the Ti_2C_2 structure of Fig. 15. This

structure is appropriate for modeling Ti-C interface effects for comparison with current experiments on Ti-C superlattices.[26] The present calculations are the initial stage of our theoretical-computational modeling study. We first examine this Ti_2C_2 lattice by taking the relatively large separation between carbon layers of 4.5 a.u., which gives a carbon-carbon distance of 5.61 a.u. This choice follows directly from assuming the dominance of the Ti—C covalent bonds and so is the natural extension of the series of lattice structures examined up to this point. This choice is also the appropriate one to explore if one speculates that, in longer-period Ti-C superlattices, the interface consists of carbon covalently bonded to the titanium (in a carbide-type structure) with the remaining carbon in graphitic layers, with only weak coupling to the surface layer of carbon. (Our results, however, suggest a different interface behavior, as discussed below.)

The *l*-projected density of states for this choice of carbon separation is given in Fig. 18. The C 2*s* band is seen to be still quite narrow, although there are now two adjacent carbon atoms per unit cell, and the 2*s* band is weakly split into molecular bonding and antibonding orbitals. There is also the appearance of a small peak just above the main C 2*s* band. The remainder of the occupied states again have the ratio of C *p* to Ti *d* density of states and the close correlation between these densities familiar from the other carbide structures. This demonstrates that these states have a large degree of covalency. This is not surprising, of course, since each Ti atom has three C nearest neighbors, and each C three Ti nearest neighbors, and there are six valence electrons between each C-Ti pair. The unoccupied states are again of largely Ti *d* type and, as in the hexagonal structure and the Ti_2C structure, are not widely separated from the covalently bonded states. Indeed, the minimum between what we have loosely termed the covalent states and the metallic states is less pronounced here than in any of the other structures and the density of states is relatively large at 18.66 states/Ry. Also evident in this figure is the observation that all of the bands here are lower in energy, by about 0.2 Ry, relative to the muffin-tin zero than in the other structures, due to a large interstitial region of very high potential between the carbon layers. This is analogous to the formation of a large work function, or band offset, resulting from the transfer of charge from titanium atoms to carbon atoms. The potential difference between a point centered between the titanium atoms of the two titanium layers and the equivalent point centered between the carbon layers is about 0.7 Ry (9.5 eV). (For this reason the value of κ^2 for the valence band was set at the interstitial-projected kinetic energy rather than simply the interstitial-projected energy.) Finally, the calculated total energy per unit cell is -3559.1044 Ry, which is a quite large 4.09 eV/atom above that of rocksalt TiC.

Another plausible form for the structure at the interface of Ti-C superlattices is one in which the interface carbon atoms are arranged in an essentially graphitic structure, either being weakly or more strongly (although not carbidically) bound to the titanium surface. Our Ti_2C_2 allows a limited ability to test this possibility since the adjacent carbon layers are stacked in an *AB* sequence. Thus, as the carbon layers are moved toward each other they approach the two-dimensional graphite structure, although we cannot, in our unit cell, reduce the *a* lattice constant of the graphitelike carbon layer to that of bulk graphite without also reducing the *a* lattice constant of the titanium layers. Figure 19 contains the calculated projected density of states with the carbon-layer separation reduced to 1.83 a.u. (where the carbon muffin-tin spheres were nearly in contact), which gives a carbon-carbon distance of 3.81 a.u. This is still much larger than the carbon separation in graphite, which is 2.68 a.u. Here the width of the C 2*s* band has increased to over 0.35 Ry with an apparent increase in the (still small) amount of C *p* orbitals included. In addition to this, the occupied states have split into two separate bands, the lower of which is now markedly a C *p* band, although with still a significant amount of Ti *d* hybridiza-

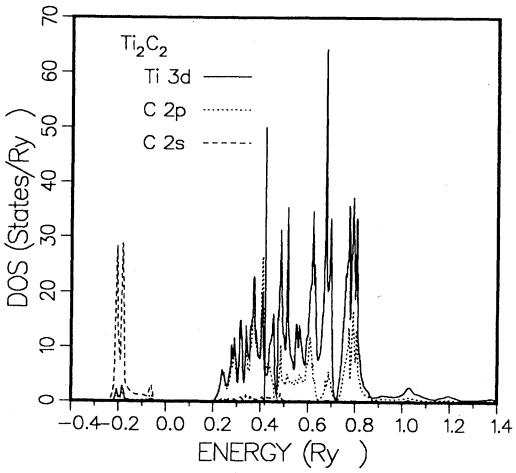

FIG. 18. Muffin-tin-sphere *l*-projected density of states for Ti_2C_2 with a distance d_3 (see Fig. 15) of 4.5 a.u. The Fermi energy is indicated by the solid vertical line.

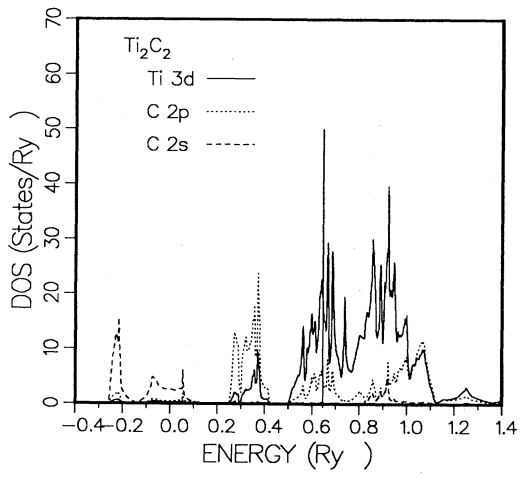

FIG. 19. Muffin-tin-sphere *l*-projected density of states for Ti_2C_2 with a distance d_3 (see Fig. 15) of 1.83 a.u.

tion. This lower band contains six of the 12 valence electrons per unit cell. The remaining occupied states are separated from these by a gap of approximately 0.1 Ry and are predominantly of Ti d character. The conclusion clearly must be that the bonding between Ti and C sites is being suppressed in favor of the formation of a p—p–bonded band of states. The total energy at this carbon-layer separation is 2.12 eV/lower than at the larger carbon-layer separation, strongly suggesting that the carbon at the interface of Ti-C superlattices is in a more graphitic structure. This agrees with the results of recent experiments.[26] Further work on this question is continuing and should be completed in the near future. Regardless of the question of the structure at the interface, is seems quite likely, from the results obtained in the Ti_2C arrangement, that additional layers of titanium quickly approach the structure and electronic behavior of bulk hcp titanium, and it also seems likely that more layers of carbon simply form as graphite.

VI. DISCUSSION

We have presented full-potential LMTO calculations of titanium-carbon systems in a variety of structures in a natural progression from the ground-state rocksalt form to very simple superlattices. The sequence of structures chosen was suggested by the fact that other carbides, especially tungsten carbides, form in related arrangements, and so we have compared TiC and WC in the two simplest of these structures. This comparison was also motivated by the desire to determine the role played by the two additional d electrons of tungsten in stabilizing these crystallographic forms, given the tendency of the metallic d levels to become occupied in the larger superlattices. For each system we have examined such quantities as the relative total energies, the equilibrium lattice constants, the electronic structure by way of the projected and total densities of states, and some of the elastic constants. We also briefly discussed larger superlattices in light of these results.

There were similarities in the electronic structure of all of the systems examined. The C $2s$ band generally remained narrow and inactive in the bonding of these lattices in each system. The one exception occurred in the Ti_2C_2 form if the carbon sites are in close contact. This system still did not exhibit promotion of a $2s$ level into the p band characteristic of carbon covalent bonding, but did appear to be approaching graphitic bond formation. Covalent M d—C p bonds were present in each system studied and were found to be an important factor in determining equilibrium lattice constants and cohesive energies. In the rocksalt structures these bonds strongly split the valence band into bonding and antibonding states with a 3–5 ratio allowing TiC to form a well-bonded structure and causing transition metals with more d electrons to be increasingly unstable in this form. In accord with this, the Fermi energy of rocksalt TiC falls at a minimum in the total density of states, while WC exhibited a relatively large density of states at the Fermi level in the rocksalt structure. The simple-hexagonal structure, while leaving the covalent p—d bonds intact, divided the metallic d levels so that the ratio of bonding to antibonding states was 4:4. This determines this hexagonal structure as the ground state of stoichiometric WC. Unlike the situation for the NaCl structure, where largely "nonbonding" d states are occupied in WC, the additional occupation of bonding d levels in hexagonal WC compared to TiC resulted in significantly different lattice constants for the two systems. In both cases the metal-carbon distance was maintained at roughly the value found in the rocksalt structure; however, in tungsten carbide the equilibrium value of c/a increased until the W-W distance became comparable to that of bulk W. Hexagonal TiC kept a c/a ratio closer to that of the cubic structure, and so had a Ti-Ti distance much smaller than in bulk Ti. For the Ti_2C lattice the covalent p—d bonds remained effective at the interface of the titanium and carbon regions, while the Ti-Ti interaction became increasingly like that in hcp bulk titanium. In Ti_2C_2 the p—d bonds were occupied when the carbon separation was kept large, but for the smaller carbon separation the p band was lowered in energy relative to the predominantly d band, resulting in a reduced amount of p-d hybridization in the occupied states.

Among the structures examined, the calculated total energies correctly predicted the ground-state form for both TiC and WC. In TiC the simple-hexagonal structure was found to lie 0.78 eV per atom above the rocksalt value, and the lower of the two Ti_2C_2 energies was 1.97 eV per atom above the rocksalt total energy. In the Ti_2C lattice, the energy per broken bond was estimated at approximately 2.8 eV. Tungsten carbide in the rocksalt form was found to have a total energy 0.26 eV per atom above that of the simple-hexagonal structure, roughly consistent with the existence of rocksalt WC above 2798 K and the observed transition from stoichiometric hexagonal WC at 3028 K.

Investigation of the 2×2 Ti_2C_2 structure was limited, but the initial results suggest that carbon at the interface has a more graphitic form of interaction and structure rather than the Ti-C covalent structure exhibited in the simple carbides. In either case, additional layers of titanium or carbon probably revert quickly to their bulk hcp or graphite forms.

ACKNOWLEDGMENTS

This research was supported by the U.S. Air Force Office of Scientific Research under Grant No. AFOSR-87-0251. We have benefited greatly from discussions with P. A. Montano and J. M. Wills.

[1]V. Ern and A. C. Switendick, Phys. Rev. **137**, 1927 (1965).
[2]R. G. Lye and E. M. Logothetis, Phys. Rev. **147**, 622 (1966).
[3]A. Neckel, P. Rastl, R. Eibler, P. Weinberger, and K. Schwarz, J. Phys. C **9**, 579 (1976).
[4]P. Blaha and K. Schwarz, Int. J. Quantum Chem. **23**, 1535 (1983).
[5]P. Blaha, J. Redinger, and K. Schwarz, Phys. Rev. B **31**, 2316 (1985).
[6]W. A. Harrison and G. K. Straub, Phys. Rev. B **36**, 2695 (1987).
[7]P. Marksteiner, P. Weinberger, A. Neckel, R. Zeller, and P. H. Dederichs, Phys. Rev. B **33**, 812 (1986).
[8]J. Redinger, R. Eibler, P. Herzig, A. Neckel, R. Podloucky, and E. Wimmer, J. Phys. Chem. **46**, 383 (1985); **47**, 387 (1986).
[9]T. W. Barbee, Jr. and J. H. Underwood, Opt. Commun. **48**, 161 (1983); Y. Lepetre, R. Rivoira, R. Philip, and G. Rasigni, *ibid.* **51**, 127 (1984); Y. Lepetre and G. Rasigni, Opt. Lett. **9**, 433 (1984); E. Ziegler, Y. Lepetre, I. K. Schuller, and E. Spiller, Appl. Phys. Lett. **48**, 1354 (1986).
[10]L. E. Toth, *Transition Metal Carbides and Nitrides* (Academic, New York, 1971).
[11]R. V. Sara, J. Am. Ceram. Soc. **48**, 251 (1955).
[12]O. K. Anderson, Phys. Rev. B **12**, 3060 (1975).
[13]H. J. F. Hansen and A. J. Freeman, Phys. Rev. B **30**, 561 (1984); L. F. Mattheiss and D. R. Hamann, *ibid.* **33**, 823 (1986).
[14]D. D. Koelling and B. N. Harmon, J. Phys. C **10**, 3107 (1977).
[15]F. S. Ham and B. Segall, Phys. Rev. **124**, 1786 (1961).
[16]D. J. Chadi and M. L. Cohen, Phys. Rev. B **8** 5747 (1973).
[17]D. M. Ceperley and B. J. Alder, Phys. Rev. Lett. **45**, 566 (1980).
[18]J. P. Perdew and A. Zunger, Phys. Rev. B **23**, 5048 (1981).
[19]M. Weinert, J. Math. Phys. **22**, 2433 (1981).
[20]G. P. Srivastava, J. Phys. A **17**, L317 (1984).
[21]M. Weinert, E. Wimmer, and A. J. Freeman, Phys. Rev. B **26**, 4571 (1982).
[22]G. Gilat and N. R. Bharatiya, Phys. Rev. B **12**, 3479 (1975).
[23]A. Dunand, H. D. Flack, and K. Yvon, Phys. Rev. B **31**, 2299 (1985).
[24]H. J. Goldschmidt, *Interstitial Alloys* (Butterworths, London, 1967).
[25]E. S. Alekseev, R. G. Arkhipov, and S. V. Popova, Phys. Status Solidi **110**, K151 (1982); L. F. Mattheiss and D. R. Hamann, Phys. Rev. B **30**, 1731 (1984).
[26]N. Thangprasert, P. A. Montano, D. L. Price, B. R. Cooper, E. Ziegler, I. K. Schuller, Y. Chan, S. S. Jin, D. Yan, and P. Lesser, Mater. Res. Soc. Proc. **122**, 589 (1988); Y. L. Chan, P. A. Montano, N. Thangprasert, D. L. Price, B. R. Cooper, E. Ziegler, I. K. Schuller, H. S. Jin, D. Yan, and P. Lesser, *ibid.* (to be published).